

Spectroscopic study of nonthermal plasmas

R. Bartiromo, F. Bombarda, and R. Giannella

*Associazione EURATOM-ENEA sulla Fusione, Centro Ricerche Energia Frascati,
Comitato Nazionale per la Ricerca e per lo Sviluppo dell'Energia Nucleare e delle Energie Alternative,
Casella Postale 65, I-00044 Frascati, Roma, Italy*

(Received 9 November 1984)

The line ratio of a dielectronic satellite to the main optically allowed line in Fe XXV has been measured in plasma discharges with a non-Maxwellian electron distribution such as those produced in tokamaks at low electron density or during heating experiments by means of Landau damping of electromagnetic waves launched into the plasma. The effect of nonthermal electrons has been clearly established in a series of experiments performed in the Frascati tokamak FT and the expressions for line intensities in these plasma conditions have been worked out. A data-analysis procedure is also presented which can give quantitative information about the nonthermal-electron content in the plasma.

I. INTRODUCTION

Nowadays tokamak devices are routinely filled with hydrogen plasmas whose central electron temperature is well inside the keV range. Under these conditions high-Z impurity atoms extracted from the limiter or the walls of the vacuum chamber become highly stripped as they penetrate in the plasma core and radiate a substantial amount of x-ray photons in the form of narrow spectral lines.

Although this represents an undesired energy loss from the plasma, often the quantity of impurities is so low that this effect is harmless for the plasma performances. Still, the photon flux is high enough to allow accurate measurements of the spectral emission which can be exploited for the diagnostic of the plasma.

A considerable amount of information can be obtained in this way as the soft-x-ray spectrum emitted by high-Z, highly stripped ions in a hot plasma, is very rich in spectral lines.¹ In fact, beside the usual electron-impact excitation of resonance lines, two other mechanisms of line formation become effective in these conditions, namely, the dielectronic recombination of free electrons and the collisional excitation of inner-shell electrons, both leading to the emission of satellite lines which are only slightly displaced in wavelength from the main optically allowed line.²

In this situation, besides the line shapes from which the plasma ion temperature can be inferred,³ it is easy to measure line-intensity ratios accurately; in fact, owing to the small spectral separation of the lines, the relative calibration of the experimental apparatus at different wavelengths is not needed. These ratios have important applications in plasma diagnostic because the different excitation mechanisms of the lines imply a different dependence of the line intensities from plasma parameters.²

A considerable amount of theoretical⁴⁻⁷ and experimental⁸⁻¹² work has been carried out in recent years on this subject, owing to the importance of this diagnostic

method for both laboratory and astrophysical plasmas, as it has been shown that information about the ionization equilibrium and the plasma electron temperature can be obtained from the line ratios.² In particular very detailed calculation of the atomic physics underlying the data interpretation have passed severe experimental tests, especially for dielectronically excited lines.⁹ Most of the work cited has dealt with Maxwellian plasmas; very recently, however, interest has arisen for the application of this method to plasma departing from the thermal equilibrium such as those produced in low-density tokamak discharges or during lower-hybrid current drive experiments.

In this paper we present an experimental study of line intensities in non-Maxwellian plasmas and a theoretical analysis aimed at the exploitation of the experimental data for a quantitative diagnostic of the nonthermal part of the distribution function. In Sec. II the influence on the line intensity of the electron distribution function is discussed. In Sec. III we present the experimental data taken in low-density tokamak discharges in the Frascati tokamak FT as well as a sample of the results obtained during lower-hybrid electron heating experiments. In Sec. IV the expressions for line intensities are revisited in order to give generalized formulas which can be applied for non-Maxwellian plasmas. In Sec. V we try to exploit our data for obtaining a quantitative estimate of the nonthermal electron content in the plasma. A discussion of the results is also presented.

II. PHYSICAL PRINCIPLES

It was pointed out by Gabriel and Phillips¹³ that different parts of the electron distribution function are responsible for the impact excitation of the optically allowed line and the dielectronic excitation of a satellite line. For a He-like ion, dielectronic satellites are emitted in a radiative transition of the kind

$$1s2pnl \rightarrow 1s^2nl,$$

where the upper level is populated through the radiationless capture of a free electron by the He-like ion in a reac-

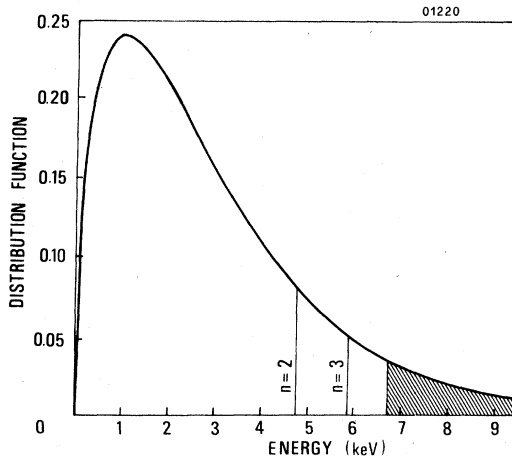
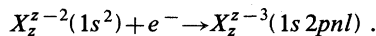


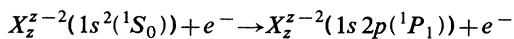
FIG. 1. Electron energies responsible for the excitation of different spectral lines of Fe XXV are shown on a Maxwellian energy distribution function with $kT_e = 2$ keV. The vertical bars represent the excitation of $n=2$ and $n=3$ dielectronic satellites. The dashed area represents the excitation of the optically allowed line.

tion of the kind



A key feature of this phenomenon is that only electrons whose kinetic energy is equal to the energy difference E_s between the Li-like excited state and the ground state of the recombining ion participate in the reaction.¹³ In other words only a thin band (whose width is related to the excited-level lifetime) of the electron distribution function is responsible for the excitation of each one of the different dielectronic satellites.

From this point of view there is a remarkable difference with electron-impact excitation of the optically allowed line



which can be excited by all the electrons having a kinetic energy greater than the transition energy E_0 .

The situation is depicted in Fig. 1 where the vertical lines represent the portions of the electron distribution function which are responsible for the dielectronic excitation of satellites with the spectator electron in different quantum states and the dashed area is the part of the distribution function which is relevant to the collisional excitation of the allowed line. The involvement of different portions of the electron distribution function makes it easy to understand the strong electron temperature dependence of the line ratio² but it is evident that, if a high-energy tail is present, the intensity of the optically allowed line is enhanced and the line ratio is lowered with respect to its expected thermal value.

The observation of this effect in a tokamak plasma has already been reported in a study of the intensity ratio of a $n=3$ dielectronic satellite to the resonance line in the He-like ion Cr XXIII.¹⁴ It is the aim of this paper to study in detail this effect both theoretically and experimentally in order to obtain more quantitative information on the departure from thermal equilibrium of the electrons in a

plasma. The heliumlike ion Fe XXV was chosen for this study since very accurate calculations of the relevant atomic physics parameters are available for it.⁴

III. EXPERIMENTAL RESULTS

The measurements have been carried out on the FT tokamak which is a high toroidal magnetic field device and is therefore well suited to the study of nonthermal effects. In fact high toroidal field tokamaks have the highest current density and enter more easily in the slide-away regime.¹⁵

Furthermore, during some of these experimental runs, a lower-hybrid heating system was used to study the interaction of the launched waves with the electrons in the plasma. In these experiments the power of the waves was damped through Landau interaction onto fast electrons inducing an important high-energy tail in the electron distribution function.¹⁶

The spectra have been recorded with a Johann spectrometer¹⁷ which has been designed for the maximum throughput in order to follow the time evolution of the discharge. A detailed description of the instrument can be found elsewhere.¹⁸

An example of the results obtained is shown in Fig. 2 where the spectrum between 1.858 and 1.848 Å is displayed. The wavelength region which can be sampled simultaneously is limited by the geometry of the access to the plasma, which is very small in the toroidal direction.

For this reason we chose to use for this study $n=3$ dielectronic satellites (A , B , and d_{13} in Fig. 2) which are sufficiently close to the optically allowed line w so that all four lines can be recorded simultaneously. The wavelengths of the lines have been obtained from the spectrometer dispersion assuming the wavelength of the w line equal to the theoretical value of 1.8500 Å (Refs. 19–21).

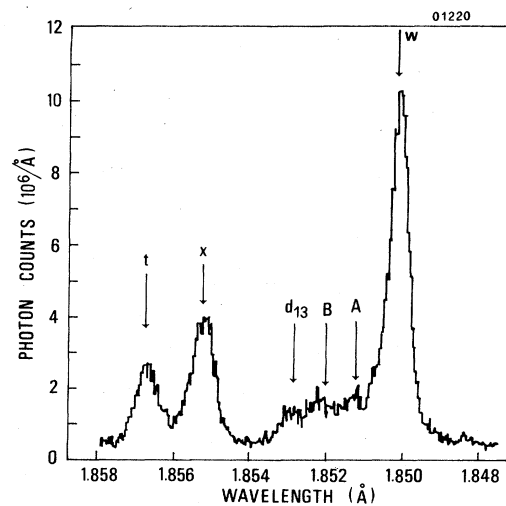


FIG. 2. Soft-x-ray spectrum around the main optically allowed line w of Fe XXV. The arrows indicate the line central wavelengths. A , B , and d_{13} are mainly $n=3$ dielectronic satellites. For a description of x and t transitions, see Ref. 4.

They are in close agreement with other determinations.^{8,9}

In principle the spectra that we collect are integrated along the line of sight of the spectrometer; however in our typical discharge condition the electron temperature is lower than 2 keV and both the He-like ion density and the excitation coefficient of the lines are peaked at the center of the plasma column and a significant photon flux is only emitted in a narrow region around the hottest plasma point.

In the data analysis for the evaluation of the line ratios, the intensity of the w line is obtained from a Gaussian fit to the experimental data, its line shape being mainly determined by Doppler broadening. For the intensity of the satellites we adopted the following procedure: first we sum all the counts from the long-wavelength end of d_{13} (1.8538 Å) up to the peak of the A line (1.8512 Å); then we subtract from this value the background measured at the short-wavelength side of the w line and the residual contribution of the w line as evaluated from the line fit. In this way the total intensity of d_{13} and B satellites plus half the intensity of the A satellite is obtained.

From a theoretical point of view the intensity of a dielectronic satellite in a thermal plasma is given by²

$$I_s(f) = 3.3 \times 10^{-24} n_e n_{\text{He}} (E_{\text{H}}/kT_e)^{3/2} F_2(s) \times \exp(-E_s/kT_e) \text{ cm}^{-3} \text{ s}^{-1},$$

where n_e and n_{He} are, respectively, the electron and the He-like ion density, and $E_{\text{H}} = 13.6$ eV is the Rydberg constant. $F_2(s)$ is a line-dependent parameter and is equal to $g_s A_a(s) A_r(s \rightarrow f) / A_{\text{tot}}(s)$, where $A_a(s)$ and $A_{\text{tot}}(s)$ are, respectively, the autoionization rate and the total decay rate of the upper level, $A_r(s \rightarrow f)$ is the radiative decay rate within the channel $s \rightarrow f$ corresponding to the line considered, and g_s is the statistical weight of the upper level of the transition.

The value of E_s is the same for all the $n = 3$ lines and is equal to 5.815 keV for FeXXV. The value of $F_2(s)$ for each of the lines involved in the A , B , and d_{13} satellites can be found in Ref. 5.

The intensity of the line w is given by

$$I_w = n_e n_{\text{He}} Q_w(T_e),$$

where $Q_w(T_e)$ is the line excitation rate and is given as a function of the electron temperature in Ref. 4. However, when the experimental line ratio is compared to the theoretical determination, the contribution of the dielectronic satellites which are blended with the w line must be taken into account. This has also been evaluated in Ref. 5.

The theoretical value R_{theor} of the dielectronic satellites to the optically allowed line w intensity ratio is a function of the electron temperature only. A point which is worth stressing here is that the atomic-physics parameters which are relevant in the calculation have already been accurately tested in a tokamak plasma.⁹

Thus from a comparison of the experimental line ratio R_{expt} to the theoretical curve, it is possible to deduce the

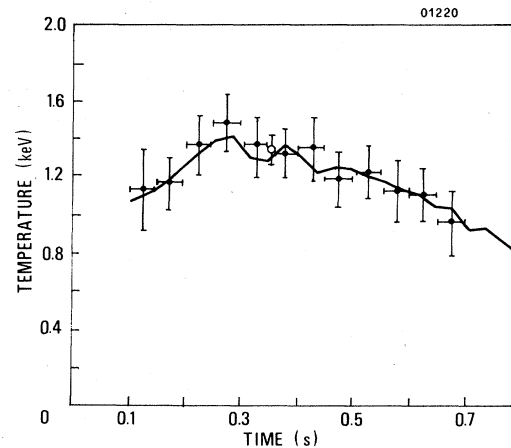


FIG. 3. The time evolution of the electron temperature measured by electron cyclotron emission diagnostic (continuous line) and the Thomson scattering value (open dot) are compared with data points (crosses) obtained from the line ratio. The discharge considered has a central electron density of $2.0 \times 10^{14} \text{ cm}^{-3}$ and 6-T toroidal magnetic field.

electron temperature at the center of the plasma discharge. The results obtained for a high-density discharge in FT are shown in Fig. 3 where it is possible to notice the good agreement with the Thomson scattering value and with the time evolution of the electron cyclotron emission diagnostic. This gives us a good level of confidence in the procedure of data analysis adopted. However when low-density discharges are analyzed, we notice that the experimental line ratio R_{expt} is systematically lower than the theoretical value R_{theor} expected from the Thomson scattering temperature.

At present we have not found any instrumental effect which could account for this phenomenon. Spatial inhomogeneities in the plasma are ruled out, too, as they should produce an R_{expt} higher than R_{theor} at the discharge center. Recalling the discussion in the previous section our results should be regarded as the evidence of a high-energy distortion in the electron distribution function.

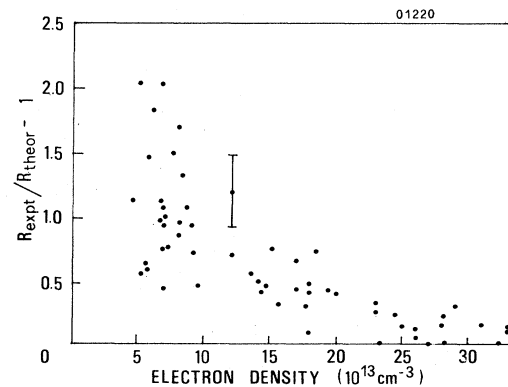


FIG. 4. The deviation of the experimental line ratio R_{expt} from its theoretical value R_{theor} as a function of the central electron density for a set of 8-T discharges. A typical error bar is also reported.

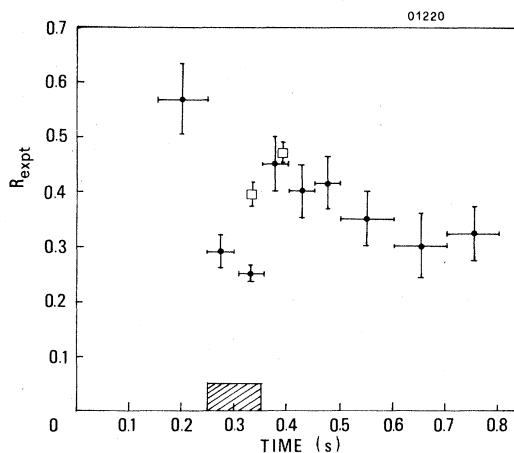


FIG. 5. The behavior of the line ratio during the rf heating pulse. The crosses represent the experimental values, the open squares the values obtained from the electron temperature measured by Thomson scattering. The dashed rectangle represents the time duration of the 130-kW heating pulse. Data obtained in a discharge at 4 T and $\bar{n}_e \sim 3 \times 10^{13} \text{ cm}^{-3}$ in FT.

In a first experiment we used the quantity $R_{\text{theor}}/R_{\text{expt}} - 1$ for a qualitative evaluation of the amount of the distortion and we studied the behavior of Ohmically heated plasmas in a systematic way. The results obtained for a set of discharges with toroidal magnetic field $B_T = 8 \text{ T}$ are plotted in Fig. 4 and show an increasing disagreement with the theoretical spectra as the electron density is decreased. We interpret this as due to a nonthermal-electron population. The amount of this effect is rather insensitive to the value of the toroidal plasma current, but is strongly enhanced when B_T is increased. A weak dependence upon the nature of the working gas has also been measured, the effect with deuterium being higher than with hydrogen.

In a second experiment we studied the evolution of the experimental line ratio in the presence of lower-hybrid heating. The results obtained are shown in Fig. 5 where it can be noticed that the line ratio nearly halves during the heating pulse where it is considerably lower than the expected thermal value, while reasonable agreement is obtained elsewhere in the discharge. This kind of effect has been noticed only during the heating of discharges whose electron density is such that the predominant interaction of the launched waves occurs with plasma electrons.²²

IV. LINE INTENSITIES

For a more quantitative analysis of the data illustrated in the previous section, the theoretical expression for the line intensities should be revisited in order to obtain more general expressions valid also for the case of plasmas whose electron population is far from the thermal equilibrium. The intensity of a satellite line emitted in a transition from an excited level s to a lower level f is given by²

$$I_s(f) = n_e n_{\text{He}} C_d \frac{A_r(s \rightarrow f)}{A_{\text{tot}}(s)}.$$

The dielectronic rate coefficient C_d can be derived from the autoionization decay rate $A_a(s)$ through the microreversibility principle. The following relation is easily obtained:

$$C_d = \frac{h^3 g_s}{4\pi g_1} \frac{A_a(s)}{(2m_e)^{3/2}} \frac{f(E_s)}{E_s^{1/2}},$$

where g_s and g_1 are, respectively, the statistical weight of the level s and of the He-like ion ground state, m_e is the electron rest mass, and $f(E_s)$ is the value of the electron distribution function at the energy E_s . From the previous expression, the usual formula for the thermal case is easily recovered when a Maxwellian function is assumed for $f(E)$.

The intensity of a collisionally excited line in a low-density plasma is given by

$$I_R = n_e n_{\text{He}} \langle \sigma v \rangle = n_e n_{\text{He}} \int_{E_0}^{\infty} \sigma(E) v(E) f(E) dE,$$

where σ is the cross section for the transition and v is the incident electron velocity. This expression neglects cascade contribution from higher levels, but this effect has been shown to be negligible for the optically allowed line of Fe XXV.⁴

Various detailed methods of calculation have been applied to obtain reliable values for the cross section,² but most of the computational effort has been restricted to a range of energy up to ten times the threshold as, when the electron distribution function is Maxwellian, only values of σ near the threshold are important. On the other hand, when the excitation energy is small compared to that of the incoming electron, the Coulomb-Bethe approximation accurately describes the cross section.²³ Then, for an optically allowed transition, the high-energy values of the cross section are given by

$$\sigma(E) = 4\pi a_0^2 \frac{E_H}{E_0} \frac{E_H}{E} f \ln \left[\frac{4E}{E_H} (\bar{k} a_0)^2 \left(\frac{E_H}{E_0} \right)^2 \right],$$

where a_0 is the Bohr radius, f the optical oscillator strength, and \bar{k} the cutoff momentum characteristic of the transition.²³

In order to find the energy range in which this approximation is useful and to derive the values of f and \bar{k} , we have compared this expression with recently published values of σ (Ref. 24) by means of a Fano plot. This comparison enables us to conclude that for electron energies higher than three times the excitation energy, the electron-impact cross section is well described by the Bethe-Coulomb approximation. A value of 0.744 for the optical oscillator strength, in agreement with other published values,^{25,26} and a value of $11.7/a_0$ for \bar{k} compatible with the theoretical expectation ($\bar{k} \sim Z/a_0$) are also deduced.

An important piece of physics, however, is still missing in this picture; in fact when the velocity of the incident electron increases, eventually approaching relativistic energies, the interaction through the exchange of virtual transverse photons becomes increasingly effective and the relativistic modification of the cross section should be considered.²⁷

It has been shown by Fano that the Bethe-Coulomb

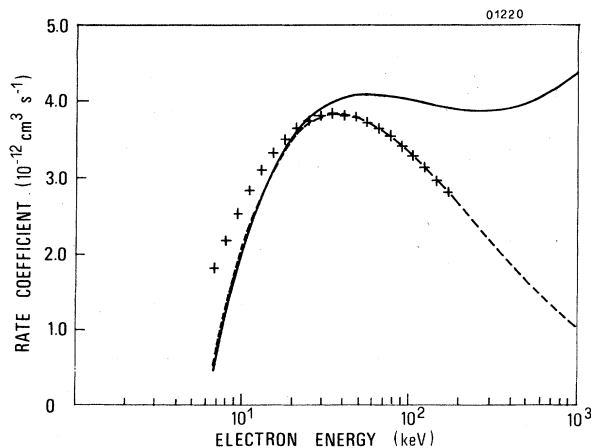


FIG. 6. The rate coefficient $\sigma(E)v(E)$ for the excitation of the $1s^2(^1S_0) \rightarrow 1s2p(^1P_1)$ transition in FeXXV is shown as a function of the electron kinetic energy E . The crosses are obtained from Ref. 24; the dashed line is the classical Coulomb-Bethe approximation; the continuous line is given by the relativistic Fano formula.

value of the cross section can still be expressed in terms of f and \bar{k} (Ref. 23):

$$\sigma(E) = \frac{8\pi a_0^2 E_H^2}{mv^2 E_0} f \left\{ \ln \left[\frac{\beta^2}{1-\beta^2} (\bar{k}a_0)^2 \right] \times \left[\frac{E_H}{E_0} \right]^2 \frac{2mc^2}{E_0} \right\} - \beta^2,$$

where v is the incident electron velocity and $\beta = v/c$.

As a result of these considerations we have plotted in Fig. 6 the rate coefficient $\sigma(E)v(E)$ which enters the integral for the line intensity. There the crosses are obtained from the values of Ref. 24, and the dashed and continuous lines represent the classical and relativistic Coulomb-Bethe approximation, respectively. From this plot we can conclude that for $E \geq 20$ keV the relativistic expression for the cross section can be used, whereas at lower energies the detailed calculated value should be retained.

V. QUANTITATIVE ANALYSIS

A proper comparison with the experimental data of the expression for the line ratio which can be derived by the formulas given in the previous section would imply a detailed knowledge of the distribution function which unfortunately is not always available. A possible strategy of data analysis is suggested by an inspection of Fig. 6 which shows that the excitation rate coefficient for the w line is constant within $\pm 10\%$ for energy greater than approximately 15 keV. This implies that, when it is possible to assume that the tail in the distribution function only develops for energies larger than this value, the non-thermal excitation of the w line is only dependent upon the total number of electrons in the tail, while the dielectric satellites are well described by the thermal expres-

sion, the distribution function at the energy relevant for their excitation still being Maxwellian.

Under this hypothesis the experimental line ratio can be exploited to evaluate the fractional population of the non-thermal electrons n_T . The following expression for this parameter can be easily deduced:

$$n_T = 3.3 \times 10^{-24} \left[\frac{1}{R_{\text{expt}}} - \frac{1}{R_{\text{theor}}(T_e)} \right] \times \left[\frac{E_H}{kT_e} \right]^{3/2} F_2(s) \exp \left[\frac{-E_s}{kT_e} \right] \frac{1}{\langle \sigma v \rangle},$$

where in our case $F_2(s) = 4.7 \times 10^{14} \text{ s}^{-1}$, $E_s = 5.815 \text{ keV}$, and $\langle \sigma v \rangle \cong 4.2 \times 10^{-12} \text{ cm}^3 \text{ s}^{-1}$ from Fig. 6.

Ohmic discharges. This scheme of data analysis has been applied to the results obtained for Ohmic discharges where the high-energy electron tail is expected to develop only in the energy range where the Coulomb frictional drag is lower than the force due to the toroidal electric field ϵ which drives the plasma current. This corresponds to electron energies greater than a critical value $E_c = kT_e(\epsilon_c/\epsilon)$, where $\epsilon_c = 4\pi e^3 n_e \ln \Lambda / kT_e$,²⁸ which is not lower than 20 keV for most of our data.

In Fig. 7 we have plotted the value of the fractional tail population n_T as a function of the runaway parameter ϵ/ϵ_c for two series of discharges with B_T equal to 8 and 4 T, respectively. The most important result obtained is that the nonthermal population is not uniquely determined by the runaway parameter, but there is an intrinsic dependence upon the toroidal magnetic field, as we mentioned before. We also checked for any dependence from the plasma current but it was within the experimental error bars.

This dependence from B_T could still be understood in the framework of the classical theory of runaway production when we take into account the effect of the anomalous Doppler instability which prevents electrons

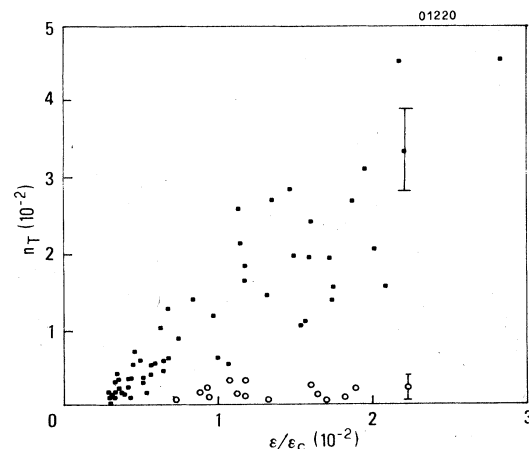


FIG. 7. The measured fractional population in the electron tail as a function of the runaway parameter. The dots refer to 8-T discharges, the open circles to 4-T discharges. Typical error bars are shown.

from reaching kinetic energies larger than $(\omega_{ce}/\omega_{pe})^3 E_c$ approximately.²⁹

However, the total amount of the suprathermal electron population can hardly be explained in terms of the classical runaway production rate. For example, if we take $\epsilon/\epsilon_c = 0.03$, the expected runaway production rate is very small ($\dot{n}_T \sim 5 \times 10^{-3} \text{ s}^{-1}$), whereas from Fig. 7, n_T is larger than 0.01 when $B_T = 8 \text{ T}$. In order to bring these two figures in agreement we should assume a very long runaway confinement time (even longer than the discharge duration).

Large nonthermal electron content with a small value of the runaway parameter has also been measured in AS-DEX (Axially Symmetric Divertor Experiment) in very low-density discharges ($n_e \leq 3 \times 10^{12} \text{ cm}^{-3}$) (Ref. 30) and in Alcator-A at densities similar to ours.^{31,32} A common feature of all these experiments is that the nonthermal phase of the discharge is characterized by a dramatic increase of high-frequency electromagnetic radiation from the plasma.³³ This observation points to an important role of wave-generation phenomena and supports the assumption that the dynamics of the suprathermal electrons is determined by their interaction with such waves.

In this perspective the role of the toroidal magnetic field can be crucial in determining the phase velocity of the generated waves as well as the energy of the particles which can interact with them.²⁹ The observation that n_T is lower in hydrogen discharges than in deuterium ones can also be understood, the faster hydrogen ions absorbing the electromagnetic power more easily than deuterium ions with the same energy.

Lower-hybrid discharges. In the case of lower-hybrid heated discharges it is expected from the theory that a plateau is established along the toroidal direction on the high-energy side of the electron distribution function through the Landau interaction of the launched waves with resonant electrons. The location of this plateau is determined by the minimum and maximum phase velocity of the waves spectrum.¹⁶

If we assume that such a spectrum is determined by the spatial periodicity of the waveguide array used to couple the electromagnetic power to the plasma, the suprathermal electron tail should only develop for energy larger than 30 keV in our experimental conditions.

However, there is enough evidence that this is not the case.^{34,35} An explanation for this observation is given by the possibility that the phase-velocity spectrum changes as the waves penetrate toward the plasma center. There are many possible causes for this effect and this point is the subject of current investigations.^{36,37} However, it is a common feature of all theoretical models aiming at an explanation of the existing experimental data to postulate a broadening of the phase-velocity spectrum toward the low phase-velocity side at the plasma center so that even electrons with energies only a few times larger than kT_e can interact with the waves.³⁸

In this framework we have used the data shown in Fig. 5 to identify a minimum value v_1 of the parallel phase velocity in the wave spectrum at the plasma center. In order to carry out this evaluation we assume the distribution function from the unidimensional quasilinear theory.¹⁶

$$f(v_{\parallel}, v_{\perp}) = n_e \left[\frac{m}{2\pi kT_e} \right]^{3/2} F(v_{\parallel}) \exp \left[-\frac{1}{2} \frac{mv_{\perp}^2}{kT_e} \right]$$

with

$$\begin{aligned} F(v_{\parallel}) &= \exp \left[-\frac{1}{2} \frac{mv_{\parallel}^2}{kT_e} \right] \text{ for } v_{\parallel} < v_1 = \frac{c}{n_1}, \\ &= \exp \left[-\frac{1}{2} \frac{mv_1^2}{kT_e} \right] \text{ for } v_1 < v_{\parallel} < v_2 = \frac{c}{n_2}, \\ &= \exp \left[-\frac{1}{2} \frac{m(v_{\parallel} - v_2 + v_1)^2}{kT_e} \right] \text{ for } v_{\parallel} > v_2. \end{aligned}$$

Here the assumption is that the electron temperature is the same in both the parallel and the perpendicular direction and is the one measured by the Thomson scattering diagnostic. The maximum value v_2 of the parallel phase velocity is determined by the requirement of accessibility to the plasma center and is equal to $c/1.7$ for the discharge considered.

Then the measured line ratio can be used to determine $n_1 = c/v_1$ from the expressions of the line intensities given in Sec. III and the distribution function given above. We have obtained $n_1 = 5.5 \pm 0.6$ which should be compared with the value calculated from the waveguide spectrum at the plasma edge which is equal to about 3.

The expression we used for the distribution function is very crude: in reality the perpendicular temperature can be very different from the parallel one and can be dependent upon the v_{\parallel} value;³⁹ nevertheless, the amount of reduction in the line ratio during the heating pulse cannot be explained without assuming an important broadening of the phase-velocity spectrum.

VI. DISCUSSION

We have shown in this paper that the presence of a high-energy component in the plasma electron distribution function can modify to an appreciable amount the intensity ratio of a dielectronic satellite to the optically allowed line of He-like iron ions. The deviation of this ratio from the theoretical value corresponding to the electron temperature of the predominant thermal bulk of the distribution function can be exploited to obtain quantitative information on the nonthermal tail when the appropriate expressions for the line intensities are taken into account.

In particular, when a model expression for the distribution function is available, the experimental value of the line ratio can be used to evaluate one of the parameters in this expression, as we have shown for the case of lower-hybrid heated discharges. On the other hand, if such a model is not available, a quantitative exploitation of the experimental data is still possible, provided that the nonthermal electrons have a minimum energy of about 15 keV; in this case their fractional density can be evaluated owing to the smooth behavior of the collisional excitation rate of the optically allowed line.

It is obviously impossible to characterize the distribution function completely in this way, even if the number of measured line ratios is increased including other satel-

lites or considering other kinds of ions. Very detailed information about the distribution function can only be obtained from measurements of the plasma bremsstrahlung emission.⁴⁰ This diagnostic, however, is very sensitive both to the energy distribution and to the distribution in angle between the direction of the electron velocity and the line of sight because of the essentially forward emis-

sion occurring at relativistic energies.

For this reason it happens that if a sufficient exploration in angle is impossible, the experimental spectra cannot be fitted unambiguously. In this respect the availability of independent information, such as those we have produced with our spectroscopic data, can be helpful in selecting the true distribution function.

- ¹C. De Michelis and M. Mattioli, *Nucl. Fusion* **21**, 677 (1981).
- ²J. Dubau and S. Volonté, *Rep. Prog. Phys.* **43**, 199 (1980).
- ³M. Bitter, S. von Goeler, R. Horton, H. Goldman, K. W. Hill, N. R. Sauthoff, and W. Stodiek, *Phys. Rev. Lett.* **42**, 304 (1979).
- ⁴F. Bely-Dubau, J. Dubau, P. Faucher, and A. H. Gabriel, *Mon. Not. R. Astron. Soc.* **198**, 239 (1982).
- ⁵F. Bely-Dubau, A. H. Gabriel, S. Volonté, *Mon. Not. R. Astron. Soc.*, **186**, 405 (1979).
- ⁶F. Bely-Dubau, J. Dubau, P. Faucher, A. H. Gabriel, M. Loulergue, L. Steenman-Clark, S. Volonté, E. Antonucci, and C. G. Rapley, *Mon. Not. R. Astron. Soc.* **201**, 1155 (1982).
- ⁷L. A. Vainshtein and U. I. Safronova, *At. Data Nucl. Data Tables* **21**, 49 (1978).
- ⁸M. Bitter, K. W. Hill, N. R. Sauthoff, P. C. Efthimion, E. Meservey, W. Roney, S. von Goeler, R. Horton, M. Goldman, and W. Stodiek, *Phys. Rev. Lett.* **43**, 129 (1979).
- ⁹M. Bitter, S. von Goeler, K. W. Hill, R. Horton, D. Johnson, W. Roney, N. Sauthoff, E. Silver, and W. Stodiek, *Phys. Rev. Lett.* **47**, 921 (1981).
- ¹⁰TFR Group, J. Dubau and M. Loulergue, *J. Phys. B* **15**, 1007 (1982).
- ¹¹F. Bely-Dubau, P. Faucher, L. Steenman-Clark, M. Bitter, S. von Goeler, K. W. Hill, C. Camhy-Val, and J. Dubau, *Phys. Rev. A* **26**, 3459 (1982).
- ¹²E. Källne, J. Källne, and J. E. Rice, *Phys. Rev. Lett.* **49**, 330 (1982).
- ¹³A. H. Gabriel and K. J. H. Phillips, *Mon. Not. R. Astron. Soc.* **189**, 319 (1979).
- ¹⁴M. L. Apicella, R. Bartiromo, F. Bombarda, and R. Giannela, *Phys. Lett.* **98A**, 174 (1983).
- ¹⁵B. Coppi, F. Pegoraro, R. Pozzoli, and G. Rewoldt, *Nucl. Fusion* **16**, 309 (1976).
- ¹⁶N. J. Fisch, *Phys. Rev. Lett.* **41**, 873 (1978).
- ¹⁷K. W. Hill, S. von Goeler, M. Bitter, L. Campbell, R. D. Cowan, B. Fraenkel, A. Greenberger, R. Horton, J. Hovey, W. Roney, N. R. Sauthoff, and W. Stodiek, *Phys. Rev. A* **19**, 1770 (1979).
- ¹⁸R. Bartiromo, R. Giannela, M. L. Apicella, F. Bombarda, S. Mantovani, and G. Pizzicaroli, *Nucl. Instrum. Methods* **225**, 378 (1984).
- ¹⁹A. H. Gabriel, *Mon. Not. R. Astron. Soc.* **160**, 99 (1972).
- ²⁰A. M. Ermolaev, M. Jones, and K. Y. S. Phillips, *Astrophys. Lett.* **12**, 53 (1972).
- ²¹U. I. Safronova, *Phys. Scr.* **23**, 241 (1981).
- ²²F. Alladio *et al.*, *Nucl. Fusion* **24**, 725 (1984).
- ²³M. Inokuti, *Rev. Mod. Phys.* **43**, 297 (1971).
- ²⁴J. B. Mann, *At. Data Nucl. Data Tables* **29**, 407 (1983).
- ²⁵A. W. Weiss, *J. Res. Natl. Bur. Stand. Sect. A* **71**, 163 (1967).
- ²⁶C. O. Lin, W. R. Johnson, and A. Dalgarno, *Phys. Rev. A* **15**, 154 (1977).
- ²⁷U. Fano, *Ann. Rev. Nucl. Sci.* **13**, 1 (1963).
- ²⁸H. Knoepfel and D. A. Spong, *Nucl. Fusion* **19**, 785 (1979).
- ²⁹V. V. Parail and O. P. Pogutse, *Nucl. Fusion* **18**, 303 (1978).
- ³⁰G. Fussmann *et al.*, *Plasma Physics and Controlled Nuclear Fusion Research 1982* (International Atomic Energy Agency, Vienna, 1983), Vol. III.
- ³¹L. Pieroni and S. E. Segre, *Phys. Rev. Lett.* **34**, 928 (1975).
- ³²J. E. Rice, K. Molvig, and H. I. Helava, *Phys. Rev. A* **25**, 1645 (1982).
- ³³A. A. M. Oomens, L. Th. M. Ornstein, R. R. Parker, F. C. Schüller, and R. J. Taylor, *Phys. Rev. Lett.* **36**, 255 (1976).
- ³⁴W. Hooke, *Plasma Phys. Controlled Fusion* **26**, 133 (1984).
- ³⁵F. Alladio *et al.*, *Plasma Phys. Controlled Fusion* **26**, 157 (1984).
- ³⁶C. S. Liu, V. S. Chan, D. K. Bhadra, and R. W. Harvey, *Phys. Rev. Lett.* **48**, 1479 (1982).
- ³⁷J. Vaclavik, K. Appert, A. H. Kritz, and L. Muschietti, *Plasma Phys.* **25**, 1283 (1983).
- ³⁸F. Santini, E. Barbato, F. De Marco, S. Podda, and A. A. Tuccillo, *Phys. Rev. Lett.* **52**, 1300 (1984).
- ³⁹C. C. F. Karney and N. J. Fisch, *Phys. Fluids* **22**, 1817 (1979).
- ⁴⁰S. von Goeler *et al.*, in *Diagnostic for Fusion Reactor Conditions*, edited by P. E. Stott, D. K. Akulina, G. G. Leotta, E. Sindoni, and C. Warton (Commission of the European Communities, Brussels, 1982), Vol. I.